

# Plugging Attention into Power Grids: Towards Transparent Forecasting

Elói Campagne<sup>1,3</sup> (✉) Itai Zehavi<sup>1,3</sup> Yvenn Amara-Ouali<sup>2,3</sup> Yannig Goude<sup>2,3</sup> Argyris Kalogeratos<sup>1</sup>

<sup>1</sup> Centre Borelli, Université Paris-Saclay, CNRS, Ecole Normale Supérieure Paris-Saclay – France<sup>†</sup>

<sup>2</sup> Laboratoire de Mathématiques d’Orsay (LMO), Université Paris-Saclay, CNRS, Faculté des Sciences d’Orsay – France<sup>‡</sup>

<sup>3</sup> EDF R&D, Palaiseau – France<sup>§</sup>

**Abstract.** Accurate electricity consumption forecasting is crucial for ensuring grid stability and optimizing power generation, particularly in increasingly decentralized and complex systems. While classical approaches such as Generalized Additive Models (GAMs) remain widely used, they often fail to capture the spatial dependencies inherent in energy networks. Graph Neural Networks (GNNs) offer a principled framework to incorporate this structure by directly leveraging graph topologies. In this work, we evaluate a broad set of GNN architectures – including GCN, GraphSAGE, ChebConv, TAG, APPNP, TransformerConv, and Graph Attention Networks (GAT and GATv2) – on two real-world electricity consumption datasets from France and the UK. Our experiments show that while complex architectures like GATv2 and TransformerConv do not consistently outperform their simpler counterparts, models such as GCN and APPNP achieve strong results in low-data or highly disaggregated settings. Nonetheless, the vanilla GAT remains highly competitive across both datasets and offers an additional interpretability layer via attention mechanisms. We perform a temporal analysis of attention weights, revealing evolving patterns of regional interaction linked to seasonal and meteorological variability. These results highlight that, although attention is not universally superior, it provides valuable explanatory power when spatial dependencies are prominent. Finally, we benchmark ensemble-based expert aggregation strategies, showing that uniform or learned combinations can enhance robustness and outperform individual models under data heterogeneity.

**Keywords:** Graph Neural Networks · Attention Mechanisms · Electricity Load Forecasting · Interpretable Machine Learning

## 1 Introduction

The effective operation of the electrical system relies on maintaining a balance between electricity supply and demand. Since electricity cannot be efficiently stored, its production needs to be constantly adjusted to match consumption. Providing accurate forecasts for short-term electricity demand is therefore crucial for all participants in the energy market. The shift toward a decentralized electricity network introduces new uncertainties, which pose additional challenges for demand forecasting. In addition, the increasing contribution of renewable energy sources, like solar and wind power, brings fluctuations and intermittency to the electricity market. These fluctuations and intermittency occur at various spatial scales due to the presence of wind farms and photovoltaic power

<sup>†</sup> Contact: {name.surname}@ens-paris-saclay.fr

<sup>‡</sup> Contact: {name.surname}@universite-paris-saclay.fr

<sup>§</sup> Contact: {name.surname}@edf.fr

plants. The crisis brought by Covid-19, along with the current economic downturn, add further complexity to forecasting due to the non-stationarity in consumption patterns [2]. The availability of new geolocated data and individual electricity consumption data can be exploited by models that are able to take advantage of additional information and help in minimizing forecast uncertainty [30, 37]. Furthermore, recent advancements in adaptive forecasting algorithms have demonstrated improvements in forecasting quality, particularly for aggregate load forecasting [3, 6].

Deep learning methods have shown great flexibility and adaptability to a wide range of problems applied to the energy sector [29]. To outperform standard methods, they usually require a large amount of data along with intricate relationships between the input features and the target. These conditions are met particularly in decentralized grids, where multiple forecasting problems can be factored with the adequate neural network architecture. Recurrent neural networks (RNNs), particularly Long Short-Term Memory (LSTM) networks, have been widely used in electricity forecasting due to their capacity to model temporal dependencies. [33] proposed a Deep LSTM model for short-term household load forecasting, which showed superior performance over traditional statistical methods such as ARIMA. Similarly, [28] developed a sequence-to-sequence LSTM model that captures the sequential nature of load data effectively. GNNs have gained significant traction for time-series forecasting tasks, due to their ability to model complex spatial-temporal dependencies. In traffic forecasting, for example, [16] proposed a spatio-temporal GNN with attention mechanisms to dynamically weigh spatial and temporal features, significantly improving predictive accuracy. Similarly, [9] developed a dynamic spatio-temporal GNN that constructs adaptive graphs to better capture temporal evolution in traffic flow. In the energy domain, [22] introduced a hybrid GNN framework for the Baidu KDD Cup 2022 wind power challenge, demonstrating the effectiveness of GNNs in modeling power-related spatial dependencies. A broader GNN-based approach was proposed by [21], where external contextual information was integrated into the model to enhance load forecasting robustness. Notably, our previous work [8] was among the first to explore GNNs specifically for electricity consumption forecasting. By leveraging graph-based representations of aggregated load data, we showed that GNNs can outperform classical baselines while revealing interpretable spatial structures across regions. Attention mechanisms have become a central component in deep learning, particularly in sequence modeling and structured data processing. Initially introduced in the context of machine translation [4, 35], attention enables models to dynamically focus on the most relevant parts of the input. In the context of graph machine learning, Graph Attention Networks (GAT) [36] extend this idea by assigning learnable weights to neighboring nodes, allowing for adaptive neighborhood aggregation. More recent variants, such as GATv2 [7] and TransformerConv [34], aim to address limitations of the original formulation by improving expressiveness or robustness. Despite their popularity, several works have raised concerns about the interpretability of attention weights [20], highlighting the need for careful evaluation when using them as explanatory tools. In this work, we leverage attention scores not only for improving predictions but also for extracting interpretable spatio-temporal patterns in power networks. These contributions highlight the promise of GNNs in energy forecasting. However, a key challenge remains: designing or inferring graph structures that are tailored to the forecasting task, rather than relying on fixed or physically-defined topologies.

In this work, we make the following contributions:

- We propose a graph-based forecasting framework for electricity consumption that integrates a broad spectrum of GNN architectures, including attention-based, diffusion-based, and spectral convolution models.

- We demonstrate that attention coefficients from GATs provide interpretable, time-varying insights into regional interactions. By applying dimensionality reduction techniques (e.g. PCA and UMAP) to sequences of attention matrices, we reveal coherent seasonal and spatial patterns aligned with physical and meteorological drivers.
- We conduct a systematic benchmark on two complementary datasets: a high-resolution UK dataset reflecting residential-level consumption, and a coarser French dataset with regional load measurements. We evaluate a wide array of GNNs, including GCN, GraphSAGE, GAT (v1/v2), TransformerConv, ChebConv, TAG, and APPNP.
- We analyze the trade-offs between model complexity, interpretability, and predictive performance, showing that simpler models such as GCN or APPNP can outperform more complex ones in low-data regimes, while attention-based models like GAT remain competitive and uniquely valuable for explainability.

## 2 Preliminaries and Background

In this section, we introduce the basics of GNNs and the various convolutions used in the study.

### 2.1 Graphs and Message Passing

Let  $\mathcal{G} = (\mathcal{V}, \mathcal{E})$  be a graph, where nodes  $v \in \mathcal{V}$  represent entities and edges  $(u, v) \in \mathcal{E}$  represent their interactions. The graph can be encoded via a binary adjacency matrix  $\mathbf{A} \in \mathbb{R}^{N \times N}$ , where  $A_{uv} = 1$  indicates an edge between  $u$  and  $v$ , or by a weighted matrix  $\mathbf{W}$  allowing finer modeling of connection strengths. The neighborhood of node  $v$  is denoted  $\mathcal{N}_v = \{u \in \mathcal{V} \mid W_{uv} > 0\}$ . GNNs rely on message passing, a core mechanism where nodes iteratively aggregate and transform information from their neighborhood. At each layer  $\ell$ , the representation  $\mathbf{h}_v^{(\ell)}$  of a node  $v$  is updated based on its own previous embedding and those of its neighbors:

$$\mathbf{h}_v^{(\ell)} = \text{UPDATE}^{(\ell)} \left( \mathbf{h}_v^{(\ell-1)}, \text{AGGREGATE}^{(\ell)} \left( \left\{ \mathbf{h}_u^{(\ell-1)} \mid u \in \mathcal{N}_v \right\} \right) \right), \quad \mathbf{h}_v^{(0)} = \mathbf{X}_v, \quad (1)$$

where AGGREGATE typically involves a permutation-invariant function (e.g. **sum**, **mean**, **max**) and UPDATE applies a nonlinear transformation. Stacking  $d$  layers allows each node to access information from its  $d$ -hop neighborhood. This framework can be interpreted as a generalization of convolution to graph structures: message passing acts as a graph convolution operator [26], extracting local features while respecting the graph topology. This relational inductive bias enables GNNs to capture complex dependencies and structural patterns, making them well-suited for learning tasks on graph-structured data, such as node classification or forecasting over spatial networks [10].

### 2.2 Graph Convolutions

**GCN.** The Graph Convolutional Network (GCN) [24] generalizes classical convolutions to non-Euclidean domains by aggregating feature information from local neighborhoods via the normalized adjacency matrix. This model is computationally efficient and provides a solid baseline for many graph learning tasks. However, its expressiveness is limited due to the fixed nature of the aggregation scheme and its inability to distinguish structural roles. The update rule is:

$$\mathbf{h}_v^{(\ell+1)} = \sigma \left( \sum_{u \in \mathcal{N}_v} \frac{1}{\sqrt{|\mathcal{N}_u|} \sqrt{|\mathcal{N}_v|}} \mathbf{W}^{(\ell)} \mathbf{h}_u^{(\ell)} + \mathbf{b} \right).$$

**GraphSAGE.** GraphSAGE (SAmple and aggreGatE) [17] is an inductive GNN framework that learns a function to generate node embeddings by sampling and aggregating features from a node's

local neighborhood. Its ability to generalize to unseen nodes makes it especially suitable for dynamic or large graphs. The choice of aggregation function significantly impacts performance; we use the max-pooling aggregator in our experiments. Its update rule is:

$$\mathbf{h}_v^{(\ell+1)} = \sigma \left( \mathbf{W}^{(\ell)} \left[ \mathbf{h}_v^{(\ell)} \parallel \max_{u \in \mathcal{N}_v} \left\{ \sigma \left( \mathbf{W}_{\text{pool}} \mathbf{h}_u^{(\ell)} + \mathbf{b} \right) \right\} \right] \right),$$

where  $[\cdot \parallel \cdot]$  is a concatenation operator.

**GAT.** The Graph Attention Network (GAT) [36] incorporates an attention mechanism to assign different weights to different neighbors during message passing. This allows the model to learn the relative importance of neighboring nodes dynamically, offering better performance on heterogeneous graphs. However, GAT suffers from training instability and increased computational cost due to multi-head attention. The node update is defined as:

$$\mathbf{h}_v^{(\ell+1)} = \left\| \sum_{k=1}^K \sigma \left( \sum_{u \in \mathcal{N}_v} \alpha_{uv}^{(k)} \mathbf{W}^{(k)} \mathbf{h}_u^{(\ell)} + \mathbf{b} \right) \right\|,$$

where the attention coefficients  $\alpha_{uv}^{(k)}$  are computed via a softmax over neighbors based on a shared attention mechanism, and  $K$  is the number of attention heads.

**GATv2.** GATv2 [7] extends GAT by improving the expressiveness of the attention mechanism. It overcomes the static linear projection limitation of the original GAT by allowing the attention score to depend on both the source and target features after the linear transformation. This offers improved flexibility and results in many tasks. The node update remains similar to GAT, with the attention score computed as:

$$\alpha_{uv}^{(k)} = \text{softmax}_u \left( \text{LeakyReLU}((\mathbf{a}^{(k)})^\top \mathbf{W}^{(k)} [\mathbf{h}_v \parallel \mathbf{h}_u]) \right).$$

**TransformerConv.** TransformerConv [34] adapts the Transformer architecture to graph data by using masked self-attention, restricting the attention mechanism to a node's local neighborhood. This approach combines the benefits of global attention with graph topology, allowing richer contextual representations. While powerful, it requires careful regularization and is more computationally demanding. The update rule is:

$$\mathbf{h}_v^{(\ell+1)} = \sigma \left( \sum_{u \in \mathcal{N}_v} \text{softmax}_u \left( \frac{(\mathbf{Q} \mathbf{h}_v^{(\ell)})^\top (\mathbf{K} \mathbf{h}_u^{(\ell)})}{\sqrt{d}} \right) \mathbf{V} \mathbf{h}_u^{(\ell)} + \mathbf{b} \right),$$

where  $\mathbf{Q}$ ,  $\mathbf{K}$ , and  $\mathbf{V}$  are learnable projection matrices.

**TAGConv.** The Topology Adaptive Graph Convolutional Network (TAGConv) [12] uses a fixed-size filter constructed from powers of the adjacency matrix to capture multi-hop neighbor information. It provides a balance between spectral and spatial approaches and performs well on graphs where neighborhood depth is important. However, the fixed propagation depth may limit its flexibility. Its update rule is:

$$\mathbf{h}_v^{(\ell+1)} = \sigma \left( \sum_{k=0}^K \left( \mathbf{D}^{-1/2} \mathbf{A} \mathbf{D}^{-1/2} \right)^k \mathbf{h}_v^{(\ell)} \mathbf{W}_k \right),$$

where  $K$  is the number of hops and  $\mathbf{W}_k$  are learnable weights.

**ChebConv.** ChebConv [11] approximates spectral convolutions using Chebyshev polynomials of the graph Laplacian. It allows for localized filters with adjustable receptive fields. Its main limitation lies in its dependency on spectral properties, which may not generalize well across different graph structures. The update rule is:

$$\mathbf{h}_v^{(\ell+1)} = \sigma \left( \sum_{k=0}^K T_k(\tilde{\mathbf{L}}) \mathbf{W}_k \right),$$

where  $T_k$  are Chebyshev polynomials and  $\tilde{\mathbf{L}}$  is the scaled Laplacian, with  $T_0(\tilde{\mathbf{L}}) = \mathbf{h}_v^{(\ell)}$  and  $T_1(\tilde{\mathbf{L}}) = \tilde{\mathbf{L}}\mathbf{h}_v^{(\ell)}$ .

**APPNP.** The Approximate Personalized Propagation of Neural Predictions (APPNP) [15] decouples feature transformation from information propagation by applying a fixed personalized PageRank diffusion [31] to the output of a neural network. This design mitigates the risk of over-smoothing often encountered in deep message passing networks and improves the model’s stability, particularly in transductive and semi-supervised learning scenarios. After computing an initial node embedding via a multilayer perceptron  $\mathbf{H}^{(0)} = \text{MLP}(\mathbf{X})$ , the node features are propagated through the graph using the iterative update rule:

$$\mathbf{h}_v^{(\ell+1)} = \sigma \left( (1 - \alpha) \sum_{u \in \mathcal{N}_v} \hat{A}_{uv} \mathbf{h}_u^{(\ell)} + \alpha \mathbf{h}_v^{(0)} + \mathbf{b} \right), \quad (2)$$

where  $\hat{\mathbf{A}} \in \mathbb{R}^{n \times n}$  denotes the symmetrically normalized adjacency matrix with added self-loops, and  $\alpha \in [0, 1]$  is the teleport (or restart) probability that controls the strength of the personalized component in the propagation. In our application, we omit the MLP transformation and directly set  $\mathbf{H}^{(0)} = \mathbf{X}^4$ , i.e. the initial node features, which simplifies the architecture while preserving the core propagation mechanism of APPNP.

### 3 Developing Robust Models with GNNs

This section presents our methodology for building robust GNNs for load forecasting: from the inference of suitable graphs, to the explanation of the forecasts obtained by the models.

#### 3.1 Inferring Graphs from Data

**Geographical Data.** To capture the relationships between the nodes of a graph, a first approach is to study the similarity matrix of the geographical positions of these nodes. Let the kernelized geodesic distance between nodes  $u$  and  $v$  be  $\mathbf{d}(u, v) := \exp \left\{ -\frac{\text{dist}(u, v)^2}{\sigma_b^2} \right\}$ , where  $\text{dist}(u, v)$  is the geodesic distance and  $\sigma_b$  is the kernel bandwidth. Then, we define the weight matrix as follows:

$$\mathbf{W}_\lambda = (\mathbf{W}_{uv})_{u, v \in \mathcal{V}} = \mathbf{d}(u, v) \cdot \mathbf{1}\{\mathbf{d}(u, v) \geq \lambda\}. \quad (3)$$

In practice,  $\lambda$  is picked such that the graph induced by  $\mathbf{W}_\lambda$  is minimally connected, and  $\sigma_b$  is set equal to the median pairwise geodesic distance. Other heuristics can be used to calculate the bandwidth of the Gaussian kernel, but in practice this one gives good results and is robust to outliers [14, 27]. Note that this approach does not take geographic distances into account: we are using a simple approach here, but we could consider reducing the weights of regions separated by physical obstacles (sea, mountains, etc.).

<sup>4</sup> Pytorch Geometric/APPNP

**Electricity and Weather Data.** Another way of capturing relationships between nodes is to exploit their spatio-temporal characteristics, particularly those known to influence electricity consumption, such as temperature, cloud cover, or directly the load signal. In practice, to construct the graph, we aggregate the normalized features by region, resulting in  $n$  matrices of dimension  $d \times T$ , where  $n$  is the number of nodes,  $d$  the number of features, and  $T$  the number of time steps. Rather than applying a dimensionality reduction technique, such as the singular value decomposition (SVD) used in [8], we retain only the most informative signal –the electricity load– to represent each region. This yields a global matrix of dimension  $n \times T$  that captures the temporal dynamics of consumption across nodes and serves as a basis for subsequent graph construction algorithms.

In this study, we evaluated three approaches for constructing the weight matrix based on the temporal similarity of regional load signals. The first method computes the Dynamic Time Warping (DTW) distance between regions using the FastDTW algorithm [32], which provides an efficient approximation with linear time and memory complexity. The second method relies on the empirical Pearson correlation matrix computed over the same time-series, where higher correlations suggest stronger connectivity. Finally, the third method uses the inverse of the covariance matrix –known as the precision matrix– which captures partial correlations and is particularly useful for identifying conditional dependencies between nodes. Each of these approaches yields a weighted adjacency matrix that can be used to define the graph structure for subsequent learning.

### 3.2 Explainability

In [8], the GNNExplainer algorithm has been used for the identification of compact subgraphs that best explain the model’s predictions, by maximizing the mutual information between the explanatory subgraph and the forecast. In this work, we adopt a complementary approach based on the analysis of attention weights over time. These weights, defined for each pair of nodes, provide an interpretable proxy for the flow of information across the graph. Considering the questions put by prior work on the reliability of attention weights as faithful explanations [20], we do not treat them as definitive indicators of causal influence. Instead, we study the distribution of attention matrices projected into lower-dimensional spaces (via PCA and UMAP) under varying meteorological conditions. This approach enables us to reveal recurrent patterns of regional similarity and detect shifts in interaction structures across seasons.

## 4 Experiments

In this section, we outline the experimental procedure used to assess GNNs, covering everything from dataset preparation to result analysis, including model parameterization.

### 4.1 Datasets

**French Dataset.** We evaluate GNN models on regional electricity consumption data provided by RTE (Réseau de Transport d’Électricité), the French electricity transmission system operator. The dataset spans from January 2015 to December 2019 and includes various features relevant to electricity demand and meteorological conditions across French administrative regions. Calendar-related features include a trend index, multiple date encodings, month and year indicators, time-of-day and day-of-year information, week numbers, day type (weekday, weekend, public holiday), specific holiday periods (e.g. Christmas, summer, national holidays), and a daylight saving time indicator. The target variable is the national electricity load (in megawatts). We also include lagged consumption features, as detailed in Sec. 4.2.

**UK Dataset.** The UK dataset<sup>5</sup> consists of aggregated half-hourly residential electricity consumption data collected via smart meters by four UK Distribution Network Operators (DNOs). Currently, data are available from the two largest DNOs, Scottish and Southern Electricity Networks (SSEN) and National Grid Electricity Distribution (NGED), covering approximately 2 million smart meters, 120,000 low voltage feeders, and 50,000 substations, starting from January 2024 (NGED) and February 2024 (SSEN), with updates subject to publication delays of 5 to 30 days. The data primarily cover regions such as Northern Scotland, the Midlands, South Wales, South West England, and Southern England. In our experiments, we use only calendar-based features (e.g. day of the week, time of day) and lagged consumption values, consistent with the setup used for the French dataset. The target variable corresponds to the electricity demand measured at residential substations.

**Synthetic Dataset.** In order to analyze the behavior and interpretability of attention weights in GATs, we generate synthetic datasets specifically designed for structural analysis rather than forecasting performance. Each dataset consists of  $N$  time-series, one per node in the graph, defined as the sum of a smooth trend, a periodic component, and additive high-frequency noise. The noise is intentionally strong to prevent models from simply fitting the individual signals, thereby encouraging the discovery of meaningful cross-node dependencies. To simulate interactions between nodes, we transform the original input signals  $\mathbf{X} \in \mathbb{R}^{T \times N}$  by  $\mathbf{A}\mathbf{X}^\top$ , where  $\mathbf{A} \in \mathbb{R}^{N \times N}$  is a coupling matrix. The supervised learning objective is to reconstruct these signals from the initial inputs. This ensures that the predictive performance essentially hinges on leveraging the coupling structure implicitly embedded in the data. We construct three variations of synthetic data:

- In the single coupling setting, a fixed, sparse, full-rank matrix  $\mathbf{A}$  is used at every time step, and no additional input is provided.
- In the explicit switching setting, two distinct coupling matrices  $\mathbf{A}_1$  and  $\mathbf{A}_2$  are used at different time steps, with a binary input indicating the active matrix (1 for  $\mathbf{A}_1$ , 0 for  $\mathbf{A}_2$ ). The switching signal is generated as a binary random vector of length  $T$ , where each value is independently drawn from a uniform distribution over  $\{0, 1\}$ . This results in a stochastic alternation between  $\mathbf{A}_1$  and  $\mathbf{A}_2$  at each time step (e.g. 0101110101001).
- In the ambiguous switching setting, the same alternation between  $\mathbf{A}_1$  and  $\mathbf{A}_2$  is used, but the model is now provided with two input categorical variables that only jointly (hence indirectly) encode which coupling matrix is in effect each time. Specifically, under  $\mathbf{A}_1$ , the pair takes a value of either (0, 0) or (1, 1) at random, while under  $\mathbf{A}_2$ , the pair takes a value of either (0, 1) or (1, 0) at random. This design ensures that each individual variable is uninformative on its own, and only their joint value contains the relevant information about the active coupling. This setup creates ambiguity, mimicking real-world latent factors that are not directly observable.

## 4.2 Experimental Settings

We consider a multivariate regression setting in which the objective is to forecast the electricity consumption for each node over the course of the following day, based on the features observed during the current day. The model takes as input a sequence of feature vectors covering the past 48 half-hour intervals and predicts the consumption values for the next 48 intervals that corresponds to the next day’s demand profile.

**Training Procedure.** Let  $\mathbf{X} \in \mathbb{R}^{n \times d \times T}$  denote the input tensor of historical node features, and let  $\mathbf{y} \in \mathbb{R}^{n \times T}$  represent the corresponding target values, where  $n \in \mathbb{N}$  is the number of nodes in the graph,  $d \in \mathbb{N}$  is the number of features per node, and  $T \in \mathbb{N}$  is the total number of time steps. Prior

<sup>5</sup> <https://weave.energy/>

to training, each input channel is normalized to the range  $[0, 1]$ , and the resulting scaled version is denoted by  $\tilde{\mathbf{X}}$ . We formulate the forecasting task as a sequence-to-sequence regression problem, where the objective is to predict the next 48 time steps based on the past 48 observations. More formally, given the input sequence  $\tilde{\mathbf{X}}_{t-48:t-1} := \{\tilde{\mathbf{X}}_\tau\}_{t-48 \leq \tau \leq t-1}$ , the model outputs predictions  $\hat{\mathbf{y}}_{t:t+47} := \{\hat{\mathbf{y}}_\tau\}_{t \leq \tau \leq t+47}$  via a GNN  $\Phi_\theta$  defined over the graph  $\mathcal{G}$ , i.e.  $\hat{\mathbf{y}}_{t:t+47} = \Phi_\theta(\mathcal{G}, \tilde{\mathbf{X}}_{t-48:t-1})$ . The training objective consists in identifying the parameter set  $\theta^*$  that minimizes the mean squared error (MSE) loss function  $\ell$ , formally:  $\theta^* \in \arg \min_\theta \ell(\Phi_\theta(\mathcal{G}, \tilde{\mathbf{X}}), \mathbf{y}) = \frac{1}{T} \sum_{t=1}^T \sum_{i=1}^n (y_{i,t} - \hat{y}_{i,t})^2$ . The parameters are optimized using mini-batch stochastic gradient descent with the Adam optimizer [23], which provides adaptive learning rates and momentum-based updates for improved convergence.

**Baseline models.** We evaluated three baseline forecasting strategies to predict the aggregated electricity demand at multiple consumption nodes. The first approach trains a separate feedforward neural network for each node to forecast the next 48 half-hourly values (i.e. the next day), using all available information up to time  $t - 1$ . The second baseline is a classical statistical method: we fit 48 independent SARIMA models per node – one for each half-hour slot – using only historical values (lags), without any exogenous covariates. This approach follows standard practices in time-series modeling that emphasize seasonality and decomposition [5]. The third baseline is a simple yet competitive persistence method, where the forecast for each time slot is directly copied from the same half-hour either on the previous day ( $D-1$ ) or the previous week ( $D-7$ ), a common benchmark in load forecasting studies [18]. These baselines provide a diverse set of references spanning machine learning, statistical, and naive forecasting paradigms.

**Evaluation Metrics.** We evaluate forecasting performance using two standard loss functions: Mean Absolute Percentage Error (MAPE) and Root Mean Square Error (RMSE). MAPE offers an interpretable percentage-based error metric, useful for comparing across scales:

$$\text{MAPE}(\mathbf{y}, \hat{\mathbf{y}}) = \frac{1}{T} \sum_{t=1}^T \left| \frac{\sum_{i=1}^N y_{i,t} - \hat{y}_{i,t}}{\sum_{i=1}^N y_{i,t}} \right| \quad \text{RMSE}(\mathbf{y}, \hat{\mathbf{y}}) = \sqrt{\frac{1}{T} \sum_{t=1}^T \sum_{i=1}^N (y_{i,t} - \hat{y}_{i,t})^2} \quad (4)$$

RMSE penalizes large deviations and is suited for assessing critical errors in load prediction [19].

**Parametrization.** To ensure fair and performant comparisons across the studied graph-based architectures, we optimized the model hyperparameters using the Optuna library [1]. The search space included core architectural parameters common to all models, such as the number of layers, the number of hidden channels per layer, the batch size, and the learning rate. Each of these plays a distinct role: `n_layers` controls the receptive field and model depth, `hidden_channels` regulates the model capacity, `batch_size` affects the training stability and generalization, and `lr` determines the speed and stability of convergence. We further included model-specific parameters to adapt the search space to each architecture. For spectral and spatial methods, such as ChebConv and TAGConv, we optimized the neighborhood order (e.g. Chebyshev polynomial degree or number of hops), which modulates the locality of the convolutional filters. For attention-based models such as GAT and TransformerConv, we additionally tuned the number of attention heads, which controls the diversity of subspaces in which attention scores are computed. For APPNP, we included the number of propagation steps  $K$ , which determines the extent of information diffusion, and the teleport (or restart) probability  $\alpha$ , which balances the trade-off between local propagation and retention of the original signal. All experiments were performed using early stopping based on validation loss, and each configuration was evaluated through multiple runs. This principled tuning



procedure enabled the selection of performant and robust architectures across both datasets. It is also important to note that the graph construction methods differ across datasets: in the French dataset, regional aggregation allows for the meaningful use of spatial graphs informed by physical proximity or meteorological similarity. In contrast, for the UK dataset – which involves highly disaggregated residential-level signals – using a fixed spatial graph can be counterproductive, as the spatial structure is weakly informative or even noisy. In this case, we relied on data-driven graph construction strategies better suited to fine-grained forecasting. The results of the optimization are reported in Table 1.

Table 1: Hyperparameters of the GNN models for the French and the UK dataset.

Dataset	Model	Graph structure	batch_size	n_layers	hidden_channels	lr	Other HP
	GCN	Space	16	1	170	$3 \cdot 10^{-3}$	None
	SAGE	Correlation	16	2	401	$4 \cdot 10^{-4}$	None
	GAT	GL3SR	16	3	364	$1 \cdot 10^{-3}$	heads = 2
	GATv2	Space	16	2	359	$4 \cdot 10^{-4}$	heads = 2
	Transformer	DistSplines	16	1	335	$3 \cdot 10^{-3}$	heads = 2
	TAG	DTW	16	3	329	$3 \cdot 10^{-4}$	$K = 1$
	Cheby	DistSplines	16	1	249	$6 \cdot 10^{-4}$	$K = 3$
	APPNP	Space	16	1	106	$2 \cdot 10^{-3}$	$(K, \alpha) = (1, 0.93)$
	GCN	Correlation	128	1	96	$5 \cdot 10^{-3}$	None
	SAGE	Correlation	32	5	207	$7 \cdot 10^{-4}$	None
	GAT	Correlation	16	1	172	$3 \cdot 10^{-3}$	heads = 1
	GATv2	Precision	128	3	71	$2 \cdot 10^{-3}$	heads = 1
	Transformer	Correlation	32	5	354	$4 \cdot 10^{-4}$	heads = 1
	TAG	DTW	64	1	70	$3 \cdot 10^{-3}$	$K = 4$
	Cheby	Correlation	32	4	118	$6 \cdot 10^{-2}$	$K = 10$
	APPNP	Precision	64	3	454	$2 \cdot 10^{-2}$	$(K, \alpha) = (8, 0.85)$

**Uncertainty Quantification and Model Aggregation.** A simple yet effective way to quantify uncertainty in neural networks is to train multiple models independently with different random initializations and aggregate their predictions [25]. This approach, known as Deep Ensembles, captures epistemic uncertainty – i.e. uncertainty stemming from limited knowledge or data – by leveraging the variability in predictions induced by different parameter configurations. It is particularly well-suited when models exhibit high variance, than can happen if small amounts of data are available or the variables are highly correlated. Given that each forecasting model carries distinct strengths and inductive biases, we further exploit their complementarity through expert aggregation. In particular, we employ the ML-Poly algorithm [13], a robust online learning method that dynamically adjusts expert weights based on past forecasting performance. In our setting, aggregation is performed every 48 time steps (i.e. once per daily prediction horizon), with weights updated daily to reflect recent accuracy. Formally, for time step  $t$ , let  $x_{j,t}$  denote the forecast of expert  $j$  and  $p_{j,t}$  its weight; the aggregated prediction is given by:  $\hat{y}_t = \sum_{j=1}^K p_{j,t} x_{j,t}$  where  $K$  is the number of experts. To avoid overfitting and reduce the complexity of model selection, we also consider uniform aggregation, which consists of a simple average over all expert forecasts. Despite its simplicity, this baseline often performs competitively – sometimes even outperforming the best individual expert – thanks to the regularizing effect of ensemble averaging which reduces the variance of predictions.

### 4.3 Results

**Numerical Results.** On the French dataset, which has a coarser spatial resolution and includes more aggregated load profiles at the regional level, performance across GNN architectures is relatively homogeneous. With uniform aggregation (over 10 random initializations for each method), SAGE delivers the best RMSE (873 MW) and a competitive MAPE (1.12%), while the vanilla GAT achieves the lowest MAPE (1.11%), confirming its ability to balance expressiveness and stability. Simpler models such as GCN and TAG remain highly competitive, and the gains from more complex architectures like GATv2 and TransformerConv are marginal or even negative. These findings suggest that in moderately sized graphs with stable and aggregated targets, moderately expressive models can match or outperform more elaborate architectures, particularly when using uniform aggregation, which helps mitigate overfitting risks and reduces variance across experts. Baseline methods such as FF or SARIMA are clearly outperformed by GNNs, reaffirming the utility of leveraging graph structure in this forecasting context.

In contrast, the UK dataset is characterized by a much finer granularity and a greater number of disaggregated nodes (residential substations), where learning is more sensitive to data sparsity and noise. Under these conditions, APPNP with uniform aggregation achieves the best results, reaching the lowest MAPE (6.54%) and RMSE (12.61 MW), followed by GAT (7.79%, 14.13 MW) and SAGE (8.19%, 14.87 MW). In this data-scarce regime, complex attention-based architectures such as GATv2 and TransformerConv perform worse, likely due to their higher parameterization and the resulting overfitting. The strong performance of APPNP can be attributed to its propagation scheme with teleportation, which regularizes diffusion and stabilizes learning. GAT’s strong results confirm that attention mechanisms can still offer competitive accuracy, especially when combined with uniform averaging, which smooths predictions across models and limits overfitting. These observations reinforce the value of simple and stable GNN designs in fine-grained and noisy environments.

Overall, the results highlight the importance of architectural simplicity and strong inductive biases in low-data, high-resolution scenarios, as well as the value of graph-aware models over global baselines. Across both datasets, the choice of aggregation strategy significantly influences performance, often surpassing the differences between GNN architectures themselves. On the French dataset, the Bottom Aggregation with learned weights consistently yields the best results, achieving the lowest MAPE (1.01%) and RMSE (789 MW). This suggests that learning to combine expert predictions at the local (node) level before aggregating them captures more informative patterns than naive averaging. Similarly, on the UK dataset, where signals are more heterogeneous and data is sparser, Bottom Aggregation (learned) also outperforms other strategies with the lowest MAPE, with 7.68%, and RMSE, with 14.35 MW. This supports the idea that local aggregation provides a finer control over uncertainty and variation at the node level before summarizing across the network. In contrast, Top Aggregation – which combines predictions after summation – tends to perform worse, especially in the UK setting, likely because it neglects node-level diversity. Moreover, while uniform weighting remains competitive, particularly in simpler models, learned aggregation offers systematic gains, underlining the benefit of adaptive combination rules in ensemble-based forecasting.

**Explainability Results.** To gain interpretability from attention-based architectures, we analyze the attention weights learned by GATs. For each time step in the dataset, the model computes a full attention matrix over all pairs of regions, quantifying the relative importance of inter-nodal interactions for the prediction task. These matrices, dynamically updated across time, encode rich

Table 2: Average and best test performance per model – ‘Unif.’ indicates uniform averaging of expert predictions, ‘Agg.’ refers to online aggregation using the MLPol algorithm. ‘Bottom’ aggregation aggregates at the node level before summation, while ‘Top’ aggregation first sums expert predictions and then aggregates. ‘\*’ means the models were only ran once as as their training procedure is deterministic .

Model	French Dataset						UK Dataset					
	MAPE (%)			RMSE (MW)			MAPE (%)			RMSE (MW)		
	Avg. $\pm$ Std	Best	Avg. $\pm$ Std	Best	Avg. $\pm$ Std	Best	Avg. $\pm$ Std	Best	Avg. $\pm$ Std	Best	Avg. $\pm$ Std	Best
GCN	1.75 $\pm$ 0.51	<u>1.21</u>	1255 $\pm$ 359	<u>903</u>			9.52 $\pm$ 1.39	<u>6.91</u>	16.68 $\pm$ 2.27	<u>12.13</u>		
Unif.	1.21		895				8.63		15.09			
Agg.	1.09		839				8.51		14.91			
SAGE	<b>1.30 <math>\pm</math> 0.09</b>	<u>1.14</u>	<b>998 <math>\pm</math> 72</b>	<b>862</b>			<u>8.63 <math>\pm</math> 0.84</u>	6.95	<u>15.61 <math>\pm</math> 1.49</u>	13.10		
Unif.	1.12		873				8.19		14.87			
Agg.	1.14		898				8.07		14.85			
GAT	1.42 $\pm$ 0.23	<b>1.13</b>	1052 $\pm$ 136	<u>888</u>			10.01 $\pm$ 1.80	<u>6.59</u>	18.11 $\pm$ 2.96	<u>12.79</u>		
Unif.	1.11		883				7.79		14.13			
Agg.	1.08		871				8.29		14.72			
GATv2	1.64 $\pm$ 0.34	1.22	1165 $\pm$ 200	937			11.32 $\pm$ 1.48	8.21	20.22 $\pm$ 2.53	15.23		
Unif.	1.14		888				8.78		16.44			
Agg.	1.14		902				8.94		16.40			
Transformer	1.50 $\pm$ 0.17	1.28	1123 $\pm$ 118	950			11.93 $\pm$ 1.41	9.69	21.24 $\pm$ 2.41	16.61		
Unif.	1.14		883				8.36		15.32			
Agg.	1.15		910				8.48		15.53			
TAG	<u>1.36 <math>\pm</math> 0.17</u>	1.22	<u>1022 <math>\pm</math> 107</u>	925			10.63 $\pm$ 1.16	7.69	18.35 $\pm$ 1.81	14.21		
Unif.	1.14		884				9.23		15.79			
Agg.	1.14		881				9.41		16.19			
Cheby	<u>1.39 <math>\pm</math> 0.14</u>	1.23	<u>1036 <math>\pm</math> 91</u>	925			<u>9.49 <math>\pm</math> 1.12</u>	7.95	18.38 $\pm$ 1.83	15.66		
Unif.	1.16		878				8.60		17.23			
Agg.	1.15		876				8.93		17.37			
APPNP	1.48 $\pm$ 0.17	1.23	1091 $\pm$ 114	931			<b>8.31 <math>\pm</math> 1.53</b>	<b>6.01</b>	<b>15.41 <math>\pm</math> 2.73</b>	<b>11.01</b>		
Unif.	1.22		944				6.54		12.61			
Agg.	1.20		943				7.60		14.13			
FF	3.53 $\pm$ 0.09	3.34	2501 $\pm$ 47	2411			10.71 $\pm$ 0.40	9.83	18.48 $\pm$ 609	17.06		
SARIMA	3.29*	3.29	2653*	2653			8.06*	8.06	16.60*	16.60		
Persistence-1	5.79*	5.79	4512*	4512			8.86*	8.86	17.20*	17.20		
Persistence-7	6.03*	6.03	4656*	4656			10.19*	10.19	19.19*	19.19		
Bottom Uniform	1.06		836				8.10		14.74			
Bottom Aggregation	<b>1.01</b>		<b>789</b>				<b>7.68</b>		<b>14.35</b>			
Top Uniform	1.08		844				8.09		14.74			
Top Aggregation	1.02		817				8.33		15.04			

spatio-temporal patterns. For instance, two regions may exhibit similar attention profiles in spring and autumn due to analogous consumption behaviors, yet diverge significantly in summer or winter – particularly in regions affected by seasonal tourism. To explore the structure embedded in these matrices, we apply dimensionality reduction techniques such as Principal Component Analysis (PCA) and Uniform Manifold Approximation and Projection (UMAP). These methods are especially useful for uncovering latent patterns in high-dimensional data: PCA captures directions of maximal variance, offering a linear projection, while UMAP preserves local and global topological structures, revealing non-linear relationships. As illustrated in Fig. 3, both projections reveal

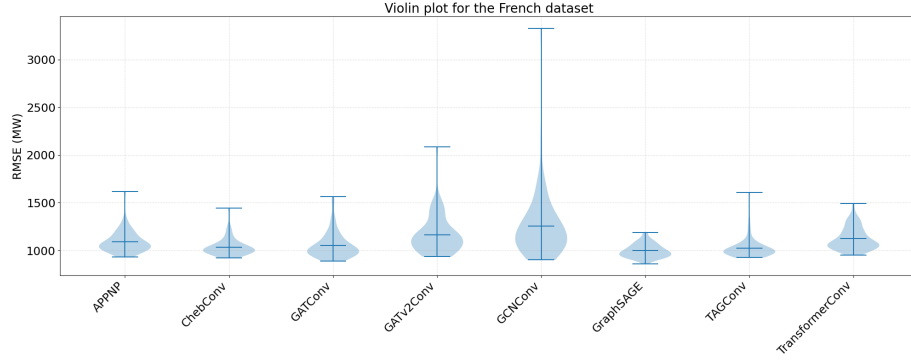


Fig. 1: Violin plot of the RMSE error values on the French dataset for the GNN models.

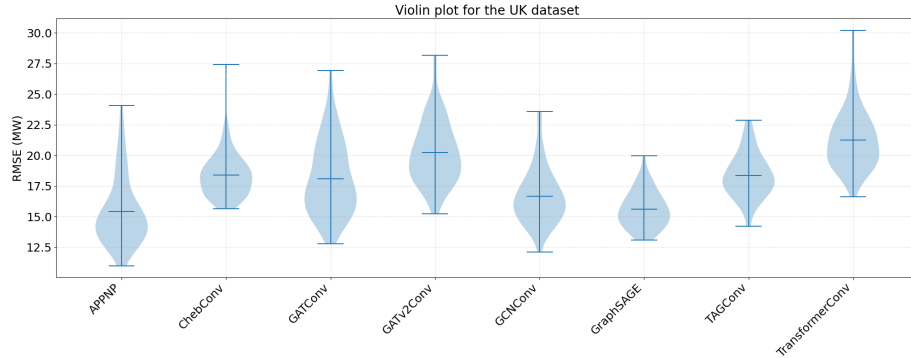


Fig. 2: Violin plot of the RMSE error values on the UK dataset for the GNN models.

a clear seasonal organization of the attention matrices. The color gradient, indicating the day of the year, reveals well-separated clusters corresponding to different periods (e.g. winter, summer). This seasonal structuring suggests that the attention mechanism implicitly captures underlying physical variables such as temperature, daylight variation, or regional activity cycles – providing an interpretable signal beyond raw consumption values. These findings reinforce the potential of attention-based models not only as powerful predictors, but also as tools for understanding spatio-temporal dynamics in energy consumption.

**Interpreting Attention on Synthetic Data.** To better understand the nature of the information captured by attention mechanisms in GATs, we conduct a series of experiments using the synthetic datasets previously described. These datasets offer controlled conditions to interpret how attention matrices reflect inter-node interactions and latent structural cues. In the single coupling scenario, where a fixed matrix  $\mathbf{A}$  governs all interactions, we observe that the average attention matrix learned by the model does not resemble the ground truth coupling matrix. Moreover, no obvious transformation seems to relate the two. This suggests that attention weights do not directly encode interpretable physical dependencies. Nevertheless, the low standard deviation of attention values across time indicates that the model learns a temporally stable pattern of interactions. To explore whether GATs can adapt to multiple interaction regimes, we consider a second scenario involving a switch between two coupling matrices,  $\mathbf{A}_1$  and  $\mathbf{A}_2$ . In the explicit switching scenario, the model

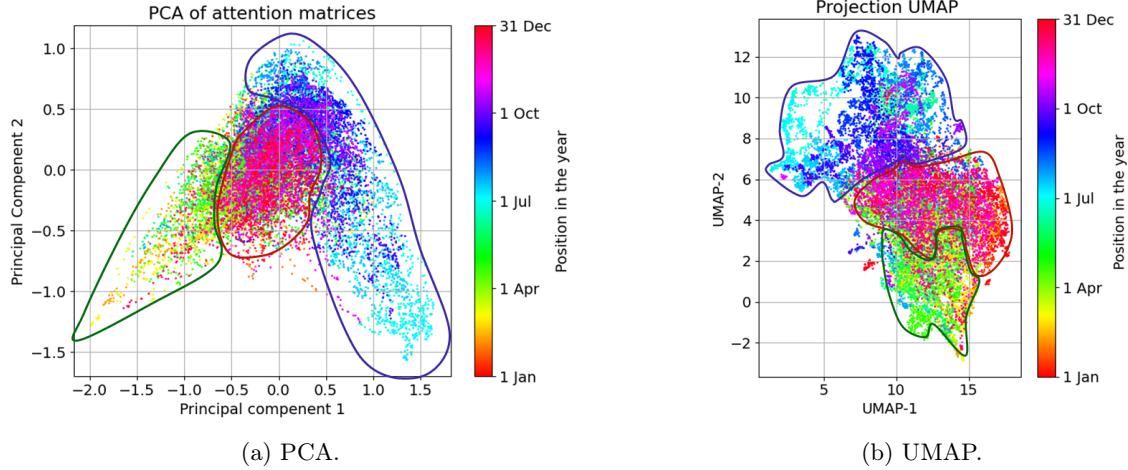


Fig. 3: PCA and UMAP projections of attention matrices on the French dataset reveal seasonal clustering: spring (green), summer (blue), and winter (red).

is given as input a binary vector indicating which of those matrices is in effect at each moment. After training, PCA is applied to the attention vectors to reveal two clearly separable clusters, as shown in Fig. 4a, demonstrating that the GAT can modulate its internal attention representations according to the active coupling mode.

To evaluate the model’s ability to recover hidden structure from ambiguous input, we design a third scenario with ambiguous switching. In this case, the same switching pattern between  $\mathbf{A}_1$  and  $\mathbf{A}_2$  is used as before, but the information about which of those matrices is in effect each time is now implicitly encoded by two categorical variables. This setup introduces ambiguity by suggesting four categories where only two actual regimes exist. We perform a PCA of the learned attention vectors at each GAT layer. As shown in Fig. 4, the first layer exhibits no clear separation. In the second layer, three intermediate clusters emerge, corresponding to the four ambiguous exogenous categories. In the final layer, these are merged into two well-separated clusters, correctly matching the underlying coupling structure. This progression suggests that GATs can disentangle latent generative factors through hierarchical attention refinement, even in the presence of misleading categorical inputs.

## 5 Conclusion

This paper investigates the use of attention-based graph neural networks for electricity consumption forecasting, with a strong focus on interpretability. We show that attention mechanisms not only improve forecasting accuracy on certain datasets, but also provide insights into time-varying regional dependencies. Our analysis of attention weight distributions reveals interpretable seasonal and meteorological patterns, which are not captured by classical black-box models. Interestingly, our results also show that simpler architectures such as GCN and APPNP often outperform deeper or more complex models (e.g. GATv2, TransformerConv), especially in highly disaggregated, low-data settings such as the UK residential network. These findings emphasize the importance of model simplicity and strong inductive biases in real-world forecasting scenarios. Finally, we show that ensemble techniques – particularly bottom-up aggregations with learned or uniform weights – offer a practical and effective strategy to improve robustness.

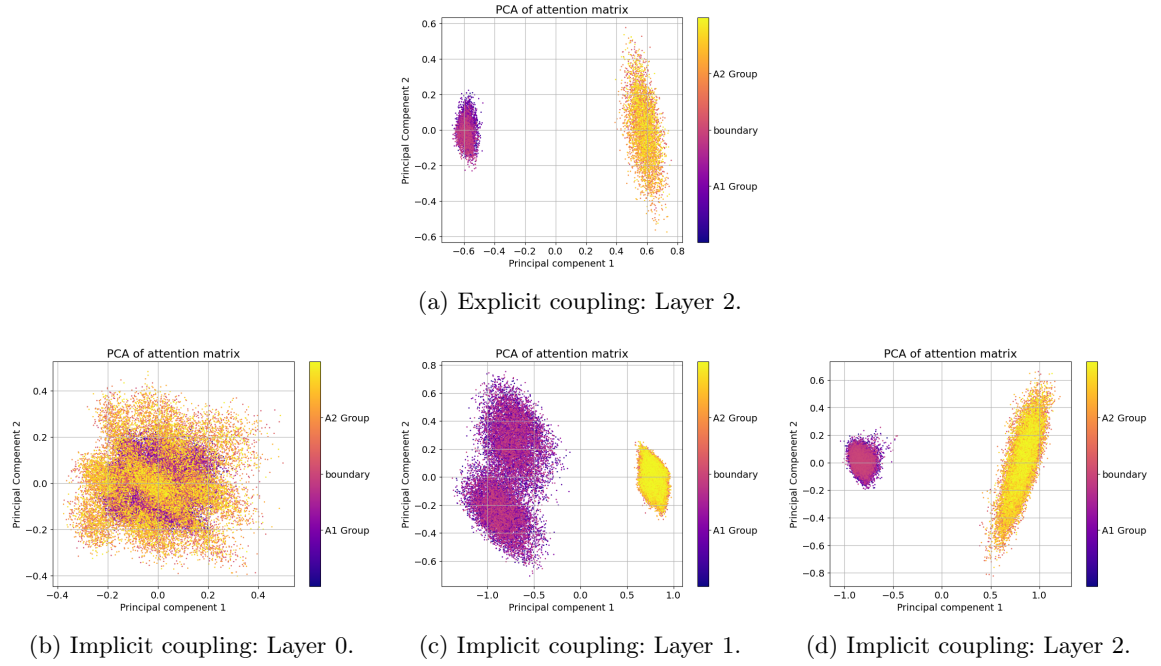


Fig. 4: PCA of attention matrices on the synthetic dataset with two coupling modes ( $\mathbf{A}_1$  or  $\mathbf{A}_2$ ). Colors reflect the coupling matrix in effect. (a) Explicit coupling information: the mode is explicitly given to the model as a binary input. (b-d) Implicit coupling information: the mode in effect is indicated implicitly by the combined values of two input binary variables. The subfigures show the PCA of attention matrices across GAT layers.

Future work may include learning graph structure jointly with forecasts and further exploring causal interpretations of attention mechanisms.

**Disclosure of Interests.** The authors have no competing interests to declare that are relevant to the content of this article.

## Bibliography

- [1] Akiba, T., Sano, S., Yanase, T., Ohta, T., Koyama, M.: Optuna: A Next-Generation Hyperparameter Optimization Framework. In: The 25th ACM SIGKDD International Conference on Knowledge Discovery & Data Mining (2019)
- [2] Alasali, F., Nusair, K., Alhmoud, L., Zarour, E.: Impact of the Covid-19 pandemic on electricity demand and load forecasting. Sustainability (2021)
- [3] Antoniadis, A., Gaucher, S., Goude, Y.: Hierarchical transfer learning with applications for electricity load forecasting (2022)
- [4] Bahdanau, D., Cho, K., Bengio, Y.: Neural machine translation by jointly learning to align and translate (2014)
- [5] Box, G.E., Jenkins, G.M., Reinsel, G.C., Ljung, G.M.: Time Series Analysis: Forecasting and Control. John Wiley & Sons (2015)
- [6] Br  g  re, M., Huard, M.: Online hierarchical forecasting for power consumption data. International Journal of Forecasting (2022)
- [7] Brody, S., Alon, U., Yahav, E.: How attentive are graph attention networks? (2021)
- [8] Campagne, E., Amara-Ouali, Y., Goude, Y., Kalogeratos, A.: Leveraging Graph Neural Networks to Forecast Electricity Consumption. In: Proceedings of the Machine Learning for Sustainable Power Systems Workshop at ECML PKDD. Vilnius, Lithuania (2024)
- [9] Chen, K., Chen, F., Lai, B., Jin, Z., Liu, Y., Li, K., Wei, L., Wang, P., Tang, Y., Huang, J., et al.: Dynamic spatio-temporal graph-based CNNs for traffic flow prediction. IEEE Access (2020)
- [10] Daigavane, A., Ravindran, B., Aggarwal, G.: Understanding convolutions on graphs. Distill (2021)
- [11] Defferrard, M., Bresson, X., Vandergheynst, P.: Convolutional neural networks on graphs with fast localized spectral filtering. Advances in neural information processing systems (2016)
- [12] Du, J., Zhang, S., Wu, G., Moura, J.M., Kar, S.: Topology adaptive graph convolutional networks (2017)
- [13] Gaillard, P., Stoltz, G., Van Erven, T.: A second-order bound with excess losses. In: Conference on Learning Theory. PMLR (2014)
- [14] Garreau, D., Jitkrittum, W., Kanagawa, M.: Large sample analysis of the median heuristic (2018)
- [15] Gasteiger, J., Bojchevski, A., G  nnemann, S.: Predict then propagate: Graph neural networks meet personalized pagerank. In: International Conference on Learning Representations (2018)
- [16] Guo, S., Lin, Y., Feng, N., Song, C., Wan, H.: Attention based spatial-temporal graph convolutional networks for traffic flow forecasting. In: Proceedings of the AAAI Conference on Artificial Intelligence (2019)
- [17] Hamilton, W.L., Ying, R., Leskovec, J.: Inductive Representation Learning on Large Graphs (2018)
- [18] Hyndman, R.J., Fan, S.: Density forecasting for long-term peak electricity demand. IEEE Transactions on Power Systems (2010)
- [19] Hyndman, R.J., et al.: Another look at forecast-accuracy metrics for intermittent demand. Foresight: The International Journal of Applied Forecasting (2006)
- [20] Jain, S., Wallace, B.C.: Attention is not Explanation. In: Proceedings of NAACL-HLT (2019)

- [21] Jiang, H., Dong, Y., Dong, Y., Wang, J.: Power load forecasting based on spatial-temporal fusion graph convolution network. *Technological Forecasting and Social Change* (2024)
- [22] Jiang, J., Han, C., Wang, J.: Buaa\_bigcity: Spatial-Temporal Graph Neural Network for Wind Power Forecasting in Baidu KDD CUP 2022 (2023)
- [23] Kingma, D.P., Ba, J.: Adam: A method for stochastic optimization (2014)
- [24] Kipf, T.N., Welling, M.: Semi-Supervised Classification with Graph Convolutional Networks (2017)
- [25] Lakshminarayanan, B., Pritzel, A., Blundell, C.: Simple and scalable predictive uncertainty estimation using deep ensembles. *Advances in Neural Information Processing Systems* (2017)
- [26] LeCun, Y., Bengio, Y., et al.: Convolutional networks for images, speech, and time series. *The handbook of brain theory and neural networks* (1995)
- [27] Long, M., Cao, Y., Wang, J., Jordan, M.I.: Learning Transferable Features with Deep Adaptation Networks (2015)
- [28] Marino, D.L., Amarasinghe, K., Manic, M.: Building energy load forecasting using deep neural networks. In: *Annual conference of the IEEE industrial electronics society* (2016)
- [29] Massaoudi, M., Abu-Rub, H., Refaat, S.S., Chihi, I., Oueslati, F.S.: Deep Learning in Smart Grid Technology: A Review of Recent Advancements and Future Prospects. *IEEE Access* (2021)
- [30] Obst, D., de Vilmares, J., Goude, Y.: Adaptive Methods for Short-Term Electricity Load Forecasting During Covid-19 Lockdown in France. *IEEE Transactions on Power Systems* (2021)
- [31] Page, L., Brin, S., Motwani, R., Winograd, T.: The pagerank citation ranking: Bringing order to the web. Tech. rep., Stanford infolab (1999)
- [32] Salvador, S., Chan, P.: FastDTW: Toward accurate dynamic time warping in linear time and space. In: *KDD workshop on mining temporal and sequential data* (2004)
- [33] Shi, H., Xu, M., Li, R.: Deep learning for household load forecasting — A novel pooling deep RNN. *IEEE Transactions on Smart Grid* (2017)
- [34] Shi, Y., Huang, Z., Feng, S., Zhong, H., Wang, W., Sun, Y.: Masked label prediction: Unified message passing model for semi-supervised classification (2020)
- [35] Vaswani, A., Shazeer, N., Parmar, N., Uszkoreit, J., Jones, L., Gomez, A.N., Kaiser, Ł., Polosukhin, I.: Attention is all you need. *Advances in neural information processing systems* (2017)
- [36] Veličković, P., Cucurull, G., Casanova, A., Romero, A., Liò, P., Bengio, Y.: Graph attention networks. In: *International Conference on Learning Representations* (2018)
- [37] de Vilmares, J., Goude, Y.: State-Space Models Win the IEEE DataPort Competition on Post-covid Day-ahead Electricity Load Forecasting (2021)